Res Chem Intermed
DOI 10.1007/s11164-015-2243-7

Synthesis, antimicrobial activity and molecular docking studies of pyrano[2,3-*d*]pyrimidine formimidate derivatives

Kotaiah Yalagala[1] · Suresh Maddila[1] · Surjyakanta Rana[1] · Surya Narayana Maddila[1] · Sukesh Kalva[2] · Adam Arnold Skelton[2] · Sreekantha Babu Jonnalagadda[1]

Received: 9 July 2015 / Accepted: 25 August 2015

Abstract A new series of ten poly-functionalized pyrano[2,3-*d*]pyrimidine formimidate derivatives were successfully synthesized. All the synthesized compounds were characterized by ^{1}H NMR, ^{13}C NMR, HRMS, and FT-IR spectral analysis. All the synthesized compounds were evaluated for their antimicrobial activity by using the well plate method and MIC by the broth micro dilution method against the strains of bacteria as well as fungus. Four compounds exhibited good to excellent antimicrobial activity. The theoretical binding mode of the target molecules was evaluated by docking studies, which revealed a new molecular scaffold for enhancing the antimicrobial activity of compounds.

Graphical Abstract Studies on synthesis, characterization, antimicrobial activity, and molecular docking of novel pyrano[2,3-*d*]pyrimidine formimidate derivatives (10) are reported. Four of the compounds exhibited excellent activity.

Electronic supplementary material The online version of this article (doi:10.1007/s11164-015-2243-7) contains supplementary material, which is available to authorized users.

✉ Sreekantha Babu Jonnalagadda
jonnalagaddas@ukzn.ac.za

[1] School of Chemistry and Physics, University of KwaZulu-Natal, Westville Campus, Chiltern Hills, Durban 4000, South Africa

[2] Discipline of Pharmaceutical Sciences, University of KwaZulu-Natal, Westville Campus, Chiltern Hills, Durban 4000, South Africa

Published online: 03 September 2015

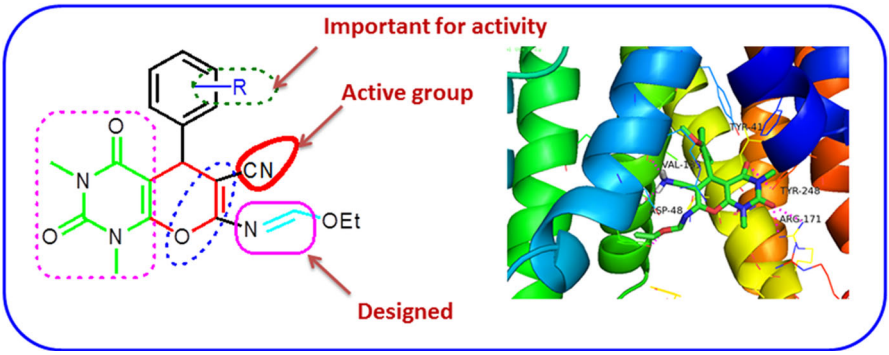

Keywords Pyrano[2,3-*d*]pyrimidine formimidates · Synthesis · Antimicrobial activity · Molecular docking studies

Introduction

Despite significant improvement in the treatment of infectious diseases caused by bacteria and fungi, it still remains a major worldwide health problem due to the rapid development of resistance against the existing antimicrobial drugs. Emerging novel antimicrobial agents with various action modes than current drugs are some of the important approaches to handle the antimicrobial resistance. In view of these facts, it is essential to develop more effective antimicrobial agents [1]. The current approach in antibacterial drug discovery is largely focused on the modification of existing classes of antibiotics. Such compounds may be prone to inactivation by existing bacterial resistance mechanisms. Therefore, in order to combat the rise and spread of antibiotic resistant strains, the discovery and development of novel classes of antibiotics, and the elucidation of their molecular targets have to be urgently pursued. Thus, the synthesis and innovation of better antimicrobial agents has been intensively sought after during the last decade.

Pyrano[2,3-*d*]pyrimidines are fused heterocyclic scaffolds that represent a privileged structural motif distributed in many naturally occurring compounds [2]. Due to their widespread assortment of pharmacological activities, these compounds received significant attention in the past few decades [3–6]. Moreover, the six membered nitrogen-containing heterocyclic compounds as fused pyranes and pyrimidines are also of biological importance due to their anti-cancer [7], antimicrobial [8], and antioxidant [9] properties. In addition, polyfunctionalized pyrano[2,3-*d*]pyrimidine derivatives are common structural subunits in a variety of important natural products [10], and they can be used as cognitive enhancers, for the treatment of neurodegenerative disorders [11]. On the other hand, the Formimidate Intermediates (FI's) play a key role in the synthesis, and these have also facilitated the production of various targeted biologically potent molecules [12]. However, the synthesis and bioactivity of the formimidate derivatives is less explored and is still attractive.

In the recent past, we have reported the synthesis and activity evaluation of various heterocyclic compounds, such as thiadiazole for anti-inflammatory activity [13], triazoles [14, 15] and 1,3,4-thiadiazoles for antimicrobial activity [16, 17]. Recently, we have also reported the computational investigation of the synthesis of pyrrole-3-carbonitriles [18]. To the best of our knowledge, there are no reports on the synthesis of pyrano[2,3-*d*]pyrimidine formimidates. In this communication, we report the synthesis of a new series of pyrano[2,3-*d*]pyrimidine formimidates and their structural evaluation. All the synthesized compounds were screened for their in vitro antimicrobial activity and molecular docking studies were implemented.

Results and discussion

Chemistry

Compounds (**4a**–**j**), amino-nitriles were prepared from aromatic aldehydes (**1a**–**j**), malononitrile (**2**), and *N,N*-dimethylbarbituric acid (**3**) with urea as a catalyst, in 1:1 mixture (v/v) of ethanol and water solvent as described in the literature [19]. Those amino-nitriles (**4a**–**j**) reacted with orthoformate to afford the target compounds (**5a**–**j**). The structures of all the products were identified and confirmed by H NMR, ^{13}C NMR, HR-MS, and FT-IR spectral analysis. The spectra data of (**5a**–**j**) showed characteristic absorption bands in the ranges between 2209 and 2218 cm^{-1} due to –C≡N stretchings. The ^{1}H NMR spectral data showed the absence of the $–NH_2$ peaks and the presence of triplets and quartets in the range between δ 1.31–1.40 and δ 4.36–4.46 for $–CH_3$ and $–OCH_2$, respectively, which were related to the ethoxy group. This strongly supports the formation of the formidates. In addition to this, there are several prominent peaks, which were related to other functional and alkyl groups that were observed. The ^{13}C NMR spectral data also reinforced the formation of the titled derivatives. Furthermore, the structures of the compounds were also confirmed on the basis of their HR-MS spectral data analysis. This evidence strongly endorses the formation of the titled compounds (Scheme 1).

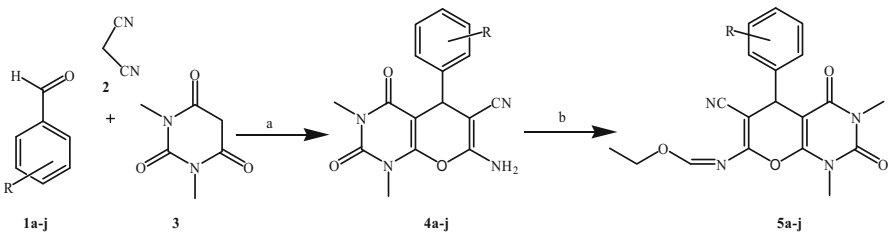

Scheme 1 Reagents and conditions: *a* 10 % Urea, EtOH:H_2O (v/v: 1:1), rt, 4 h. *b* $CH(OEt)_3$, reflux, 8 h. **R** = 2-Cl (**5a**); 2-Br (**5b**); 2-F (**5c**); 4-Cl (**5d**); 4-Br (**5e**); 4-F (**5f**); 2-OMe (**5g**); 4-OMe (**5h**); 2, 5-Di-OMe (**5i**); 2, 3-Di-OMe (**5j**)

Antimicrobial studies

In the quest for new antibacterial and antifungal agents, all the newly synthesized compounds **5a–j** were screened for their in vitro antibacterial activity against *Staphylococcus aureus*, *E. coli*, *K. pneumonia* and *P. aeruginosa* bacterial strains and in vitro antifungal activity against *A. flavus* and *C. albicans* fungal strains. The antibacterial and antifungal activities were measured by minimum inhibitory concentration (MIC) using the broth dilution method [20, 21].

During the antibacterial screening, compounds **5d**, **5f**, **5i**, and **5j** displayed significant activity against various bacterial strains. The corresponding MIC values for compounds **5d**, **5f**, **5i,** and **5j** against all the tested bacterial strains were **6.25**, **6.25**, **6.25,** and **6.25** μg $ml^{-1,}$ respectively, and values were comparable to the standard drug, ciprofloxacin. **5d**, **5f**, **5i,** and **5j** with 4–Cl, 4–F, 2,5–OMe, and 2,3–OMe groups, respectively, on the phenyl ring have exhibited good activity. Compounds **5a, 5c, 5g,** and **5h** have also exhibited moderate activity against all the tested bacterial strains, relative to ciprofloxacin. The antibacterial evaluation clearly indicates the derivatives. The results are tabulated in Table 1.

The results of antifungal activity summarized in Table 1 clearly show that **5a**, **5c**, **5g**, and **5h** have significant activity against *A. flavus* and *C. albicans* with a MIC value of **3.12** μg ml^{-1}, which is as good as to the standard drug, Fluconazole. The other derivatives showed moderate antifungal activity against all the tested microbial strains. It may be generalized from the antifungal activity that electron

Table 1 Antimicrobial activity of the compounds (**5a–j**): Minimum inhibitory concentrations (MIC)/ μg ml^{-1}

Compound	Antibacterial activity				Antifungal activity	
	S. aureus	*E. coli*	*K. pneumoniae*	*P. aeruginosa*	*A. flavus*	*C. albicans*
5a	12.5	12.5	12.5	50	12.5	6.25
5b	>100	>100	>100	>100	100	100
5c	12.5	12.5	12.5	12.5	6.25	6.25
5d	6.25	6.25	6.25	6.25	3.12	3.12
5e	N.A	N.A	N.A	N.A	N.A	N.A
5f	6.25	6.25	6.25	6.25	3.12	3.12
5g	6.25	12.5	12.5	12.5	25	25
5h	12.5	12.5	25	6.25	12.5	12.5
5i	6.25	6.25	6.25	6.25	3.12	3.12
5j	6.25	6.25	6.25	12.5	3.12	6.25
Ciprofloxacin	**3.12**	**3.12**	**3.12**	**3.12**	N.t	N.t
Fluconazole	N.t	N.t	N.t	N.t	**1.56**	**1.56**
Blank	–	–	–	–	–	–

Lower MIC values indicate higher antimicrobial activity

Bold values indicate the reference values using standard drugs

N.t Not tested, *N.A* Not Active

withdrawing and electron donating groups such as Cl, F and OMe on the phenyl ring exerted significant activity, when compared to other groups.

Molecular docking

The molecular docking studies were carried out to understand the binding mode and mechanism of active inhibitors with the crystal structure of the C(30) carotenoid dehydrosqualene synthase (PDB ID: 3ACX). Docking energy data for all the synthesized compounds along with standard ciprofloxacin is included in Table 2. Docking results show that ciprofloxacin had less docking energy compared with the new target compounds. The docking energy for all the compounds ranged from –6.43 to –10.16 kcal/mol. All the compounds could dock in the active site of dehydrosqualene synthase effectively. The binding mode of the most potent compounds **5d**, **5f**, **5i** and **5j**, is shown in Fig. 1. All the four compounds were involved in H-bonding with the active site residues Asp48, Tyr41, and His18 with the high docking energies indicating that those are directly involved in inhibiting the dehydrosqualene synthase. The binding modes of these compounds are discussed below.

Binding mode of compound 5d

Figure 1a shows the H-bond interactions with the active site residues of dehydrosqualene synthase, where NH1 and OH group of compound **5d** donates the hydrogen bond interactions with the Asp 48 and Val 133 (2.7 Å). The O4 group of compound, **5d** accepts the hydrogen bond with the NH2 group of Arg171, whereas the N4 group of compound **5d** donates the H-bond interaction with Asn168.

*Binding mode of compound **5f***

The NH1 and N4 group of compound **5f** establishes trivalent H-bond interactions with the side chain amino acid residue Asp48 and OH group of compound **5f** forms

Table 2 Docking score of the compounds (**5a–j**) and ciprofloxacin

Compounds	Docking energy (Kcal/mol)
5a	−7.27
5b	−6.42
5c	−7.57
5d	−8.91
5e	−6.91
5f	−8.50
5g	−9.28
5h	−7.01
5i	−9.48
5j	−10.16
Ciprofloxacin	−8.712

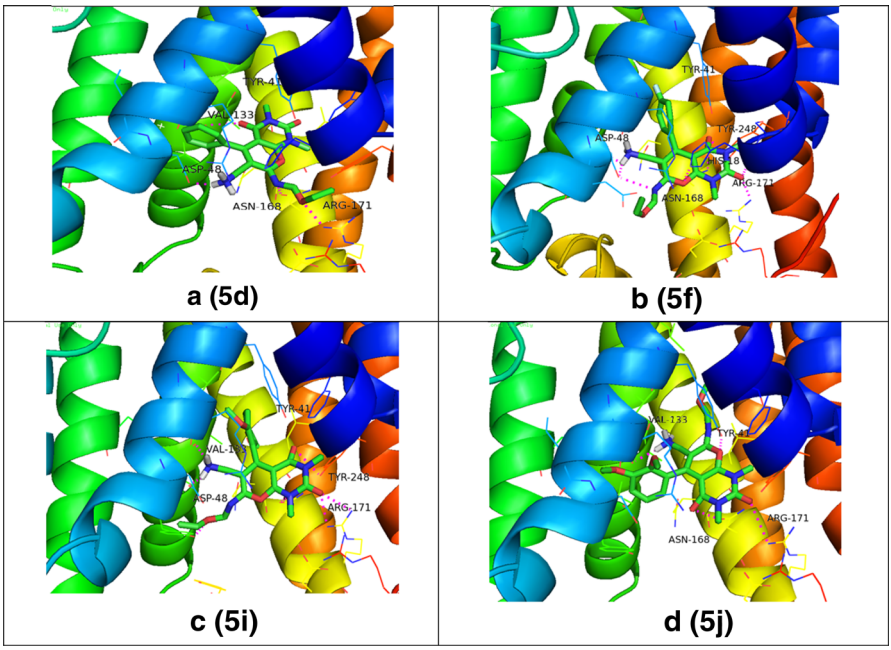

Fig. 1 Docking study of active molecules

bivalent interactions with the His 18 and Arg171. The OH and NH group of Tyr248 and Asn168 accepts the H-bond with the OH group of compound **5f** (Fig. 1b).

*Binding mode of compound **5i***

The NH1 group of compound **5i** also forms similar H-bond interactions with Asp 48 like compound **5d**, whereas the main chain amino acid residue Val133 accepts the H-bond with the N1 group of compound **5i**. The OH group of the compound shows the bivalent H-bond interaction with the side chain amino acid residue of Arg171, whereas Tyr129 forms the H-bond interaction with the O4 group of compound **5i**. The O3 and N3 groups of compound **5i** share the H-bond interactions with the side chain amino acid residues of Tyr248 and Asn168 (Fig. 1c).

*Binding mode of compound **5j***

The higher binding energy of compound **5j** indicates that this can bind more tightly with the active site residues of dehydrosqualene synthase. The O1 group of compound **5j** forms the H-bond interaction with the active site residue of Tyr41 whereas the N1 group donates the H-bond with the side chain amino acid residue of Val133. The O2 and O3 groups of the compound **5j** shares H-bond with the Arg171 and Asn168 (Fig. 1d).

Docking results infer that two oxygen atoms of 1,3-dimethylpyrimidine-2,4(1*H*,3*H*)-dione, and oxygen and one nitrile group of 4*H*-pyran-3-carbonitrile among all compounds form interactions with the active site residues of dehydrosqualene synthase. This indicates that introduction of acceptor and donor groups at that position in the moiety may enhance antimicrobial activity.

Conclusion

We have synthesized a new series of pyrano[2,3-*d*]pyrimidine formimidate derivatives and evaluated them for their in vitro antimicrobial activity. Compounds **5d**, **5f**, **5i,** and **5j** have shown significant antibacterial activity against *S. aureus*, *E. coli*, *K. pneumonia,* and *P. aeruginosa* (MIC 6.25 μg/ml) relative to ciprofloxacin. Antifungal activity data revealed that compounds **5d**, **5f**, **5i,** and **5j** exhibited excellent activity against two fungal strains, *A. flavus,* and *C. albicans* with (MIC 3.25 μg/ml). Thus, the above compounds can be considered as lead compounds for enhancing their activity and development of more potent antimicrobial agents. Furthermore, molecular docking studies revealed the essential groups, which bind with the active site of the dehydrosqualene synthase.

Experimental

Chemistry

All chemicals and reagents required for the reactions were of analytical grade, obtained from Sigma-Aldrich and were used without any further purification. A Bruker AMX 400 MHz NMR spectrometer was used to record the ^{1}H NMR and ^{13}C NMR spectral values. High-resolution mass data were obtained using a Bruker micro TOF-Q II ESI instrument operating at ambient temperature. The $CDCl_3$ solution was utilized for this while TMS served as the internal standard. TMS was further used as an internal standard for reporting the all chemical shifts in δ (ppm). The FT-IR spectrum for the samples was established using a Perkin Elmer Perkin Elmer Precisely 100 FT-IR spectrometer at the 400–4000 cm^{-1} area. Purity of all the reaction products was confirmed by TLC using aluminum plates coated with silica gel (Merck Kieselgel 60 F254).

General procedure for the synthesis of compounds **4a–j** A mixture of chosen aromatic aldehyde (**1a–j**) (1 mmol), malononitrile **2** (1.1 mmol) and urea (10 mol%) in a specific volume of equal ratio of EtOH:H_2O (1:1 v/v) was stirred at room temperature (RT) for 30 min. A solution of the *N,N*-dimethylbarbituric acid **3** (1 mmol) in ethanol (10 vol) was added to the above mixture. The resulting mixture was further stirred for 5 h at RT. The progress of the reaction was monitored by TLC. After completion of the reaction, the total mixture was poured into ice cold water, stirred for 15 min and then filtered, and solid was washed with

water (100 mL). Further, it was recrystallized by a mixture of ethanol and water (80:20) [19].

General procedure for the synthesis of target compounds **5a–j** A mixture of compound (**4a–j**) (1 mmol) and triethyl orthoformate (10 mmol) was refluxed for 8 h under inert conditions. After completing the reaction (monitored by TLC), the crude product was cooled to room temperature, and the unreacted triethyl orthoformate was evaporated under reduced pressure. The solid product obtained was recrystallized from ethanol. Structures of all the products (**5a–j**) were established and confirmed on the basis of their spectral data, ^{1}H NMR, ^{13}C NMR, HRMS and FTIR. The details of the product characterization are presented in the ESI.

(E)-ethyl-N-5-(2-chlorophenyl)-6-cyano-1,3-dimethyl-2,4-dioxo-2,3,4,5-tetrahydro-1H-pyrano[2,3-d]pyrimidin-7-ylformimidate: (**5a**) Yield: 76 %, m.p.: 208–210 °C; FTIR (Neat) υ (cm^{-1}): 2960, 2212, 1716, 1686, 1652, 1612; ^{1}H NMR (400 MHz, $CDCl_3$) δ: 1.31 (t, 3H, $J = 8.0$ Hz –OCH$_2$<u>CH$_3$</u>), 3.17 (s, 3H, CH$_3$), 3.42 (s, 3H, CH$_3$), 4.36 (q, 2H, $J = 8.0$ Hz, –O<u>CH$_2$</u>CH$_3$), 5.03 (s, 1H, –<u>CH</u>), 7.14 (dd, 1H, $J = 4.0$ Hz, Ar–<u>H</u>), 7.18 (dd, 1H, $J = 4.0$ Hz, Ar–H), 7.23 (d, 1H, $J = 4.0$ Hz, Ar–H), 7.30 (dd, 1H, $J = 8.0$ Hz, Ar–H), 8.18 (s, 1H, –N=<u>CH</u>); ^{13}C NMR (100 MHz, $CDCl_3$) δ: 13.8, 28.2, 29.6, 37.0, 65.0 (–<u>C</u>–H), 82.5, 88.2, 115.7 (–<u>C</u>≡N), 127.3, 129.3, 130.5, 133.6, 137.4, 150.3, 151.4, 155.3, 159.4 (–<u>C</u>=O), 160.7 (–<u>C</u>=O); TOF–MS–ES^{+}: $m/z = 423$ $[M + Na]^{+}$; HR–MS calcd. For 423.0836 found: 423.0843. $C_{19}H_{17}ClN_4O_4$.

(E)-ethyl-N-5-(2-bromophenyl)-6-cyano-1,3-dimethyl-2,4-dioxo-2,3,4,5-tetrahydro-1H-pyrano[2,3-d]pyrimidin-7-ylformimidate: (**5b**) Yield: 74 %, m.p.: 198–200 °C; FTIR (Neat) υ (cm^{-1}): 2953, 2209, 1712, 1682, 1656, 1610; ^{1}H NMR (400 MHz, $CDCl_3$) δ: 1.39 (t, 3H, $J = 8.0$ Hz –OCH$_2$<u>CH$_3$</u>), 3.23 (s, 3H, CH$_3$), 3.25 (s, 3H, CH$_3$), 4.42 (q, 2H, $J = 8.0$ Hz, –O<u>CH$_2$</u>CH$_3$), 5.17 (s, 1H, –<u>CH</u>), 7.15 (dd, 1H, $J = 4.0$ Hz, Ar–<u>H</u>), 7.21 (dd, 1H, $J = 4.0$ Hz, Ar–H), 7.56 (d, 1H, $J = 4.0$ Hz, Ar–H), 7.58 (dd, 1H, $J = 8.0$ Hz, Ar–H), 8.26 (s, 1H, –N=<u>CH</u>); ^{13}C NMR (100 MHz, $CDCl_3$) δ: 14.2, 28.4, 29.2, 44.4, 62.7 (–<u>C</u>–H), 82.6, 85.9, 112.6 (–<u>C</u>≡N), 125.4, 128.2, 129.8, 133.3, 134.7, 150.5, 151.6, 157.1, 160.3 (–<u>C</u>=O), 169.1 (–<u>C</u>=O); TOF–MS–ES^{+}: $m/z = 467$ $[M + Na]^{+}$, 469 $[M + 2 + Na]^{+}$; HR–MS calcd. For 467.0826 found: 467.0834. $C_{19}H_{17}BrN_4O_4$.

(E)-ethyl-N-6-cyano-5-(2-fluorophenyl)-1,3-dimethyl-2,4-dioxo-2,3,4,5-tetrahydro-1H-pyrano[2,3-d]pyrimidin-7-ylformimidate: (**5c**) Yield: 68 %, m.p.: 194–196 °C; FTIR (Neat) υ (cm^{-1}): 2962, 2211, 1714, 1680, 1653, 1613; ^{1}H NMR (400 MHz, $CDCl_3$) δ: 1.42 (t, 3H, $J = 8.0$ Hz –OCH$_2$<u>CH$_3$</u>), 3.19 (s, 3H, CH$_3$), 3.29 (s, 3H, CH$_3$), 4.46 (q, 2H, $J = 8.0$ Hz, –O<u>CH$_2$</u>CH$_3$), 5.09 (s, 1H, –<u>CH</u>), 7.10 (m, 1H, Ar–<u>H</u>), 7.24 (m, 1H, Ar–H), 7.63 (d, 1H, $J = 4.0$ Hz, Ar–H), 7.71 (dd, 1H, $J = 8.0$ Hz, Ar–H), 8.31 (s, 1H, –N=<u>CH</u>); ^{13}C NMR (100 MHz, $CDCl_3$) δ: 13.4, 28.2, 29.5, 44.1, 62.3 (–<u>C</u>–H), 83.1, 86.7, 111.9 (–<u>C</u>≡N), 124.3, 127.1, 128.9, 132.8, 133.6, 148.4, 152.8, 154.6, 162.5 (–<u>C</u>=O), 164.0 (–<u>C</u>=O); TOF–MS–ES^{+}: $m/z = 407$ $[M + Na]^{+}$; HR–MS calcd. For 407.1208 found: 407.1215. $C_{19}H_{17}FN_4O_4$.

(E)-ethyl-N-5-(4-chlorophenyl)-6-cyano-1,3-dimethyl-2,4-dioxo-2,3,4,5-tetrahydro-1H-pyrano[2,3-d]pyrimidin-7-ylformimidate: (**5d**) Yield: 81 %, m.p.: 211–213 °C; FTIR (Neat) υ (cm^{-1}): 2971, 2218, 1713, 1681, 1644, 1614; ^1H NMR (400 MHz, $CDCl_3$) δ: 1.32 (t, 3H, $J = 8.0$ Hz –$OCH_2\underline{CH_3}$), 3.19 (s, 3H, CH_3), 3.25 (s, 3H, CH_3), 4.37 (q, 2H, $J = 8.0$ Hz, –$O\underline{CH_2}CH_3$), 4.58 (s, 1H, –CH), 7.19 (d, 2H, $J = 4.0$ Hz, Ar–H), 7.25 (d, 2H, $J = 4.0$ Hz, Ar–H), 8.18 (s, 1H, –N=CH); ^{13}C NMR (100 MHz, $CDCl_3$) δ: 13.8, 28.3, 29.1, 33.0, 65.1 (–C–H), 84.1, 89.1, 115.9 (–C≡N), 129.2, 133.8, 139.5, 150.2, 150.9, 154.9, 159.3 (–C=O), 160.3 (–C=O); TOF–MS–ES^+: $m/z = 423$ $[M + Na]^+$; HR–MS calcd. For 423.0836 found: 423.0842. $C_{19}H_{17}ClN_4O_4$.

(E)-ethyl-N-5-(4-bromophenyl)-6-cyano-1,3-dimethyl-2,4-dioxo-2,3,4,5-tetrahydro-1H-pyrano[2,3-d]pyrimidin-7-ylformimidate: (**5e**) Yield: 74 %, m.p.: 208–210 °C; FTIR (Neat) υ (cm^{-1}): 2955, 2217, 1712, 1681, 1644, 1613; ^1H NMR (400 MHz, $CDCl_3$) δ: 1.32 (t, 3H, $J = 8.0$ Hz –$OCH_2\underline{CH_3}$), 3.19 (s, 3H, CH_3), 3.41 (s, 3H, CH_3), 4.37 (q, 2H, $J = 8.0$ Hz, –$O\underline{CH_2}CH_3$), 4.56 (s, 1H, –CH), 7.14 (d, 2H, $J = 8.0$ Hz, Ar–H), 7.40 (d, 2H, $J = 8.0$ Hz, Ar–H), 8.18 (s, 1H, –N=CH); ^{13}C NMR (100 MHz, $CDCl_3$) δ: 13.8, 28.3, 29.1, 38.1, 65.1 (–C–H), 84.0, 89.0, 115.9 (–C≡N), 122.0, 129.6, 132.0, 140.0, 150.9, 154.9, 159.3 (–C=O), 160.7 (–C=O) TOF–MS–ES^+: $m/z = 467$ $[M + Na]^+$, 469 $[M + 2 + Na]^+$; HR–MS calcd. For 467.0331 found: 467.0338. $C_{19}H_{17}BrN_4O_4$.

(E)-ethyl-N-6-cyano-5-(4-fluorophenyl)-1,3-dimethyl-2,4-dioxo-2,3,4,5-tetrahydro-1H-pyrano[2,3-d]pyrimidin-7-ylformimidate: (**5f**) Yield: 70 %, m.p.: 201–203 °C; FTIR (Neat) υ(cm^{-1}): 2963, 2215, 1714, 1684, 1642, 1616; ^1H NMR (400 MHz, $CDCl_3$) δ: 1.34 (t, 3H, $J = 8.0$ Hz –$OCH_2\underline{CH_3}$), 3.20 (s, 3H, CH_3), 3.40 (s, 3H, CH_3), 4.41 (q, 2H, $J = 8.0$ Hz, –$O\underline{CH_2}CH_3$), 4.62 (s, 1H, –CH), 7.18 (m, 2H, Ar–H), 7.32 (m, 2H, Ar–H), 8.20 (s, 1H, –N=CH); ^{13}C NMR (100 MHz, $CDCl_3$) δ: 13.9, 28.6, 29.4, 38.6, 65.4 (–C–H), 84.6, 88.9, 115.7 (–C≡N), 122.1, 130.2, 132.1, 139.4, 151.2, 154.5, 159.6 (–C=O), 161.3 (–C=O); TOF–MS–ES^+: $m/z = 407$ $[M + Na]^+$; HR–MS calcd. For 407.1208 found: 407.1214. $C_{19}H_{17}FN_4O_4$.

(E)-ethyl-N-6-cyano-5-(2-methoxyphenyl)-1,3-dimethyl-2,4-dioxo-2,3,4,5-tetrahydro-1H-pyrano[2,3-d]pyrimidin-7-ylformimidate: (**5g**) Yield: 67 %, m.p.: 196–198 °C; FTIR (Neat) υ (cm^{-1}): 2940, 2213, 1708, 1687, 1657, 1601; ^1H NMR (400 MHz, $CDCl_3$) δ: 1.38(t, 3H, $J = 8.0$ Hz –$OCH_2\underline{CH_3}$), 3.25 (s, 3H, CH_3), 3.49 (s, 3H, CH_3), 3.82 (s, 3H, –$O\underline{CH_3}$) 4.42 (q, 2H, $J = 8.0$ Hz, –$O\underline{CH_2}CH_3$), 4.95 (s, 1H, –CH), 6.93 (m, 2H, $J = 4.0$ Hz, Ar–H), 7.22 (dd, 1H, $J = 4.0$ Hz, Ar–H), 7.27 (m, 1H, Ar–H), 8.23 (s, 1H, –N=CH); ^{13}C NMR (100 MHz, $CDCl_3$) δ: 13.8, 28.2, 29.1, 34.1, 55.7, 64.8 (–C–H), 83.4, 88.7, 111.5, 116.3 (–C≡N), 120.9, 128.4, 129.2, 150.4, 151.4, 155.3, 157.4, 158.8 (–C=O), 161.1 (–C=O); TOF–MS–ES^+: $m/z = 419$ $[M + Na]^+$; HR–MS calcd. For 419.1331 found: 419.1339. $C_{20}H_{20}N_4O_5$.

(E)-ethyl-N-6-cyano-5-(4-methoxyphenyl)-1,3-dimethyl-2,4-dioxo-2,3,4,5-tetrahydro-1H-pyrano[2,3-d]pyrimidin-7-ylformimidate: (**5h**) Yield: 73 %, m.p.: 221–223 °C; FTIR (Neat) υ (cm^{-1}): 2946, 2209, 1711, 1682, 1651, 1604; ^1H

NMR (400 MHz, $CDCl_3$) δ: 1.40(t, 3H, J = 8.0 Hz –$OCH_2\underline{CH_3}$), 3.27 (s, 3H, CH_3), 3.51 (s, 3H, CH_3), 3.86 (s, 3H, –$O\underline{CH_3}$) 4.46 (q, 2H, J = 8.0 Hz, –$O\underline{CH_2}CH_3$), 5.02 (s, 1H, –$\underline{CH}$), 7.18 (d, 2H, J = 8.0 Hz, Ar–$\underline{H}$), 7.28 (d, 2H, J = 8.0 Hz, Ar–H), 8.20 (s, 1H, –N=$\underline{CH}$); ^{13}C NMR (100 MHz, $CDCl_3$) δ: 13.8, 28.3, 29.2, 34.3, 65.2 (–$\underline{C}$–H), 84.1, 89.6, 115.9 (–$\underline{C}\equiv$N), 121.2, 126.7, 128.4, 132.9, 141.8, 150.5, 154.8, 159.1 (–$\underline{C}$=O), 160.8 (–$\underline{C}$=O); TOF–MS–ES$^+$: m/z = 419 $[M + Na]^+$; HR–MS calcd. For 419.1331 found: 419.1337. $C_{20}H_{20}N_4O_5$.

(E)-ethyl-N-6-cyano-5-(2,5-dimethoxyphenyl)-1,3-dimethyl-2,4-dioxo-2,3,4,5-tetrahydro-1H-pyrano[2,3-d]pyrimidin-7-ylformimidate: (**5i**) Yield: 70 %, m.p.: 219–221 °C; FTIR (Neat) υ (cm^{-1}): 2955, 2211, 1697, 1667, 1634,1595; ^{1}H NMR (400 MHz, $CDCl_3$) δ: 1.38 (t, 3H, J = 8.0 Hz –$OCH_2\underline{CH_3}$), 3.26 (s, 3H, CH_3), 3.48 (s, 3H, CH_3), 3.75 (s, 3H, –$O\underline{CH_3}$), 3.79 (s, 3H, –$O\underline{CH_3}$), 4.42 (q, 2H, J = 8.0 Hz, –$O\underline{CH_2}CH_3$), 4.94 (s, 1H, –$\underline{CH}$), 6.73–6.77 (m, 2H, Ar–$\underline{H}$), 6.82 (m, 1H, Ar–H), 8.21 (s, 1H, –N=$\underline{CH}$); ^{13}C NMR (100 MHz, $CDCl_3$) δ: 13.8, 28.2, 29.0, 33.7, 55.6, 56.5, 64.8 (–$\underline{C}$–H), 83.5, 88.7, 113.0, 116.2 (–$\underline{C}\equiv$N), 130.0, 150.4, 151.4, 151.8, 153.7, 158.8 (–$\underline{C}$=O), 160.8 (–$\underline{C}$=O); TOF–MS–ES$^+$: m/z = 449 $[M + Na]^+$; HR–MS calcd. For 449.1437 found: 449.1432 $C_{21}H_{22}N_4O_6$.

(E)-ethyl-N-6-cyano-5-(2,3-dimethoxyphenyl)-1,3-dimethyl-2,4-dioxo-2,3,4,5-tetrahydro-1H-pyrano[2,3-d]pyrimidin-7-ylformimidate: (**5j**) Yield: 73 %, m.p.: 220–222 °C; FTIR (Neat) υ (cm^{-1}): 2952, 2213, 1698, 1669, 1661,1593; ^{1}H NMR (400 MHz, $CDCl_3$) δ: 1.36 (t, 3H, J = 8.0 Hz –$OCH_2\underline{CH_3}$), 3.25 (s, 3H, CH_3), 3.50 (s, 3H, CH_3), 3.78 (s, 3H, –$O\underline{CH_3}$), 3.81 (s, 3H, –$O\underline{CH_3}$), 4.41 (q, 2H, J = 8.0 Hz, –$O\underline{CH_2}CH_3$), 4.98 (s, 1H, –$\underline{CH}$), 6.69 (d, 1H, J = 4.0 Hz, Ar–$\underline{H}$), 7.12 (d, 1H, J = 4.0 Hz, Ar–H), 7.18 (d, 1H, J = 4.0 Hz, Ar–H), 8.24 (s, 1H, –N=$\underline{CH}$); ^{13}C NMR (100 MHz, $CDCl_3$) δ: 13.6, 28.1, 29.2, 34.1, 56.0, 56.8, 64.9 (–$\underline{C}$–H), 83.4, 87.2, 113.6, 117.1 (–$\underline{C}\equiv$N), 131.4, 150.2, 151.6, 152.0, 154.5, 159.2 (–$\underline{C}$=O), 161.4 (–$\underline{C}$=O); TOF–MS–ES$^+$: m/z = 449 $[M + Na]^+$; HR–MS calcd. For 449.1437 found: 449.1434 $C_{21}H_{22}N_4O_6$.

Antimicrobial activity

A microdilution broth susceptibility assay was used for the antibacterial evaluation of the compounds [20], while antifungal susceptibility of the fungus yeasts was examined according to the NCCLS reference method for broth dilution antifungal susceptibility testing of yeasts [21]. Ciprofloxacin was used as the antibacterial standard, whereas Fluconazole was used as the antifungal reference.

Molecular docking

Ligand preparation

Ligand and protein preparation were performed using the structure editing option of Chimera software [22, 23]. This module adds hydrogens and assigns Gasteriger charges for the ligands. Later each ligand was minimized for 100 minimization

steps. After ensuring that hydrogens and charges have correctly added, the ligands are saved as mol2 format.

Protein preparation

Dehydrosqualene synthase of *S. aureus* was considered as a major enzyme for the bacterium to survive inside the host cell [24]. In this study the 3-D crystal structure of dehydrosqualene synthase (PDB ID: 3ACX) complexed with inhibitor, BPH-673, was retrieved from the protein data bank to study the binding mode of inhibitors. Prior to protein preparation, the inhibitor, BPH-673, was deleted from the protein using chimera. The solvent molecules in the protein were removed, hydrogen atoms, and Kollmann charges were added using the AutoDock program. Furthermore, the protein structure was fixed and energy minimized using the steepest descent algorithm for 100 minimization steps using UCSF Chimera. The purpose of this step was to relieve bad contact involving solvent molecules in the initially solvated system [22, 23].

Receptor grid generation

A grid was generated using the Auto Dock 4.0 by selecting the active site residues in the protein dehydrosqualene synthase (PDB ID: 3ACX) [25, 26]. Active site residues of PDB ID: 3ACX to perform docking studies were chosen from the PDBsum website. Docking studies were carried out using grid sizes 48, 72, and 52 along with the x, y, and z axes with 0.375 angstroms spacing.

Docking using AutoDock

Rigid docking was performed to predict the interacting mode of a series of inhibitors with receptors using AutoDock v 4.0 [25, 26]. The ligands were docked to the receptor using the default settings of the Lamarckian genetic algorithm. After docking, the individual binding conformations of each ligand were observed, and the interactions with the protein were studied. The best and the most energetically favorable conformation of each ligand were selected based on the fitness function that was optimized by the genetic algorithm. The results of the docking studies were quantified in terms of the binding energy (kcal/mol). The predicted binding free energy was used as criteria for ranking the compounds.

Acknowledgments The authors are thankful to the School of Chemistry and Physics, University of KwaZulu-Natal, Durban, South Africa for the facilities and financial support.

References

1. C.M. Da Silva, D.L. Da Silva, L.V. Modolo, R.B. Alves, M.A. De Resende, C.V.B. Martins, A. De Fatima, J. Adv. Res. **2**, 1 (2011)

2. A. Goel, V.J. Ram, Tetrahedron **65**, 7865 (2009)
3. E.M. Grivaky, S. Lee, J. Med. Chem. **23**, 327 (1980)
4. J.A. Valderrama, P. Colonelli, D. Vasquez, M.F. Gonzalez, J.A. Rodriguez, C. Theoduloz, Bioorg. Med. Chem. **16**, 10172 (2008)
5. D. Heber, C. Heers, U. Ravens, Pharmazie **48**, 537 (1993)
6. S. Furuya, T. Ohtaki, European Patent Applications EP 608565 (1994)
7. P.K. Paliwal, S.R. Jetti, S. Jain, Med. Chem. Res. **22**, 2984 (2013)
8. S. Maddila, S.B. Jonnalagadda, Arch. Pharm. Life Sci. **345**, 163 (2012)
9. S. Maddila, A.S. Kumar, S. Gorle, M. Singh, P. Lavanya, S.B. Jonnalagadda, Lett. Drug Des. Discov **10**, 186 (2013)
10. L. Bonsignore, G. Loy, D. Secci, A. Calignano, Eur. J. Med. Chem. **28**, 517 (1993)
11. T.N. Riley, G.O. Rankin, J. Med. Chem. **19**, 334 (1976)
12. A.V. Dolzhenko, G. Pastorin, A.V. Dolzhenko, W.K. Chui, Tetrahedron Lett. **50**, 5617 (2009)
13. S. Maddila, S. Gorle, M. Singh, P. Lavanya, S.B. Jonnalagadda, Lett. Drug Des. Discov. **10**, 977 (2013)
14. S. Maddila, R. Pagadala, S.B. Jonnalagadda, Lett. Org. Chem. **10**, 693 (2013)
15. S. Maddila, S.B. Jonnalagadda, Lett. Drug Des. Discov. **9**, 687 (2012)
16. S. Maddila, S.B. Jonnagadda, Pharm. Chem. J. **46**, 1 (2013)
17. Y. Kotaiah, K. Nagaraju, N. Harikrishna, C. Venkata Rao, L. Yamini, M. Vijjulatha, Eur. J. Med. Chem. **75**, 195 (2014)
18. R. Pagadala, S.K. Kankala, S. Maddila, P. Singh, B. Moodley, N.A. Koorbanally, S.B. Jonnalagadda, Org. Biomol. Chem. **13**, 1800 (2015)
19. G. Brahmachari, B. Banerjee, ACS Sustain. Chem. Eng. **2**, 411 (2014)
20. E.W. Koneman, S.D. Allen, W.C. Winn, *Colour atlas and textbook of diagnostic microbiology* (Lippincott Raven Pub, Philadelphia, 1997), pp. 86–856
21. NCCLS, Reference method for broth dilution antifungal susceptibility testing of yeasts approved standard, second ed., ISBN: 1-56238-469-4 NCCLS document M27-A2 (2002)
22. E.F. Pettersen, T.D. Goddard, C.C. Huang, G.S. Couch, D.M. Greenblatt, E.C. Meng, T.E. Ferrin, J. Comput. Chem. **25**, 1605 (2004)
23. P.T. Lang, S.R. Brozell, S. Mukherjee, E.F. Pettersen, E.C. Meng, V. Thomas, R.C. Rizzo, D.A. Case, T.L. James, I.D. Kuntz, RNA **15**, 1219 (2009)
24. A.K. Kahlon, S. Roy, A. Sharma, J. Biomol. Struct. Dyn. **28**, 201 (2010)
25. G.M. Morris, D.S. Goodsell, R.S. Halliday, R. Huey, W.E. Hart, R.K. Belew, A.J. Olson, J. Biomol. Struct. Dyn. **19**, 1639 (1998)
26. R. Artali, G. Beretta, P. Morazzoni, E. Bombardelli, F. Meneghetti, J. Enzyme Inhib. Med. Chem. **1**, 287 (2009)